B-5.3 Mass Circulation Variations due to Seasonal and Longer Term Variations in the Middle Atmosphere Circulation

Contact Person Kiyotaka Shibata, Senior Researcher
Climate Research Department, Meteorological Research Institute
Japan Meteorological Agency
Nagamine 1-1, Tsukuba, Ibaraki, 305, Japan
Tel: +81-298-53-8602 Fax: +81-298-55-2552
E-mail: kshibata@mri-jma.go.jp

Total Budget for FY1994-FY1996 18,511,000 Yen (FY1996; 5,798,000 Yen)

Abstract Off-line transport experiments are made with general circulation models (GCMs) in order to investigate the details of the air mass inflow from the troposphere into the stratosphere in low latitudes. At first, the effect of vertical and horizontal resolutions on the simulated middle atmosphere was investigated with GCMs extending from the surface to the middle mesosphere. The numerical experiments with four GCMs (R13L23, R13L92, R24L92 and R74L92) revealed that the increase in horizontal or vertical resolution induces westerly wind in the equatorial middle stratosphere, and that the westerly region goes down similarly to the real quasi-biennial oscillation. However, there seems no downward propagation of easterly region. Next, passive-tracer transport experiments are made with R24L92 and R74L92 GCMs. 10,000 tracers, initially located in 200-150 hPa over the equator, are transported by off-line GCM winds for two-months. This experiment are made every month for 2 and half years. It is found that the tracer inflow into the stratosphere shows an anti symmetric property. In particular, major inflow occurs in southern hemisphere in northern summer and autumn. In addition, there are favorable region for the inflow, where two conditions must be satisfied simultaneously : large diabatic heating and small-circulation wind.

Key Words Middle Atmosphere, Seasonal Variations, Mass Circulation, Numerical Simulation

1. Introduction

Dissipation of eddies, propagating upward from the troposphere, in the middle atmosphere drives the mean meridional or diabatic circulation, resulting in cross-tropopause mass flux : upward flux in the tropics and downward flux in the extratropics (Holton et al., 1996). This indicates that the middle atmosphere plays an important role in the global circulation of trace gases such as ozone, ozone depleting chemicals, carbon dioxide. The detail of this circulation, however, is still not well understood partly because of the scantiness of observations. Then model simulations are expected to be a reliable tool, as a complement of observations, to investigate the global mass circulation.

This study is to explore the role of middle atmosphere on the global mass circulation by making and using general circulation models, which can well reproduce the characteristics of the middle atmosphere. This study comprises of two parts. The first is to investigate the effect of model resolution on the simulated middle atmosphere, and the other is to make off-line calculation of tracer transport experiment.

2. Model

The model used in this study is a MRI GCM (Shibata and Chiba, 1990) extending from the surface to the middle mesosphere (0.05 hPa). Simulations are made with four spectral GCMs. A control simulation is made with a R13L23 model, which is rhomboidally truncated at a wave number 13 and has a vertical resolution of 2.8 km with 23 levels. Experiment simulations are made with three GCMs, which have the same vertical resolution (grid spacing of about , 92 levels). This three GCMs are rhomboidal truncation models of R13L92, R24L92, and a parallelogramic truncation one, which is truncated zonally and meridionally at wave numbers of 13 and 74, respectively, and hence has a maximum total wave number of 87 (referred to henceforth as R74L92). The latitudinal resolutions are about 5.5 (R13), 3.0 (R 24), 1.4 (R74), respectively. Time integrations start on June 1st, when there is weak easterly wind in the equatorial lower stratosphere, and continue to about two years.

3. Effect of model resolution

In the control run the initial weak easterly wind in the equatorial lower stratosphere shows little variations throughout the entire period. In R13L92 simulation westerly wind appears in the equatorial stratosphere after two months or so, and persists between 15 and 60 hPa with a weak annual variation of its height. The peak westerly wind is about 7 m/s. In R24L92 simulation a similar evolution can be seen for the initial four months, but the westerly wind gradually lowers its top to about 20 hPa during the next five months. Though the pace slows down very much, the top height still continues to decrease to 30 hPa for about one year with a maximum wind speed of 9 m/s. In R74L92 model the westerly wind, more intensified than those in R13L92 and R24L92 models, lowers its peak height from 25 to 50 hPa during the period from the seventh to 14th month with a maximum value of about 15 m/s (Figure 1), though its top maintains nearly constant height (10 hPa). Around the 14th month the westerly wind region abruptly shrinks to about 30 hPa, and after then the westerly wind occupies nearly the same vertical extent.

Rain amounts (not shown) and mass stream functions, so long as low latitudes are concerned, do not seem to significantly differ to each other, thus indicating that the horizontal resolution does not affect so much the excitation of the equatorial waves.

A spectral analysis is made for the equatorial waves, which are thought to be responsible for the difference in the simulated equatorial stratosphere. Figure 2 shows the frequency-latitude cross section of temperature power of wave number 1 in the middle stratosphere (about 50 hPa) for the period from July to September. In R13L92 model the power of Kelvin waves are

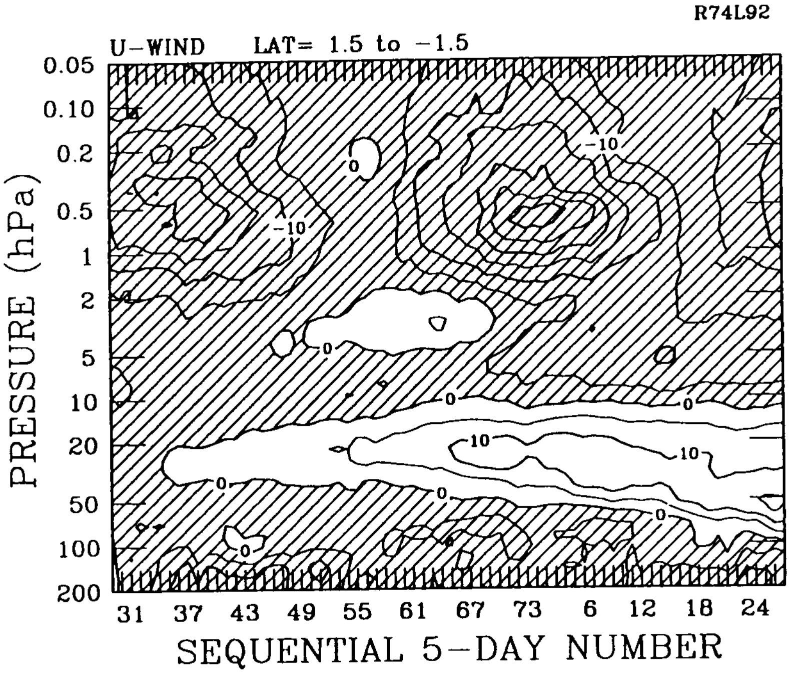

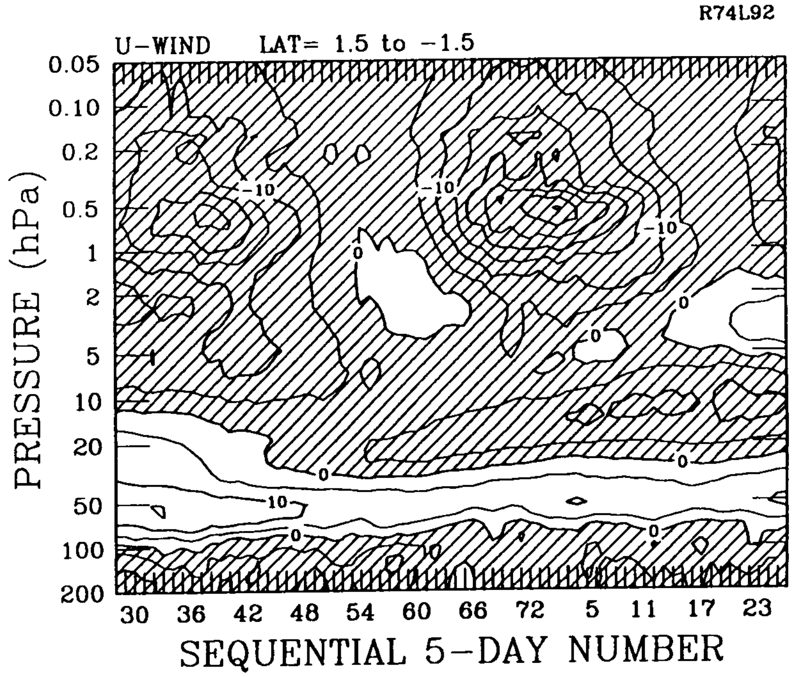

Figure 1 Time-pressure cross section of zonal mean zonal wind over the equator in R74L92 model for two year. The numbers in abscissa represent the sequential five-day number. Contour interval is 5 m/s and easterly wind regions are shaded.

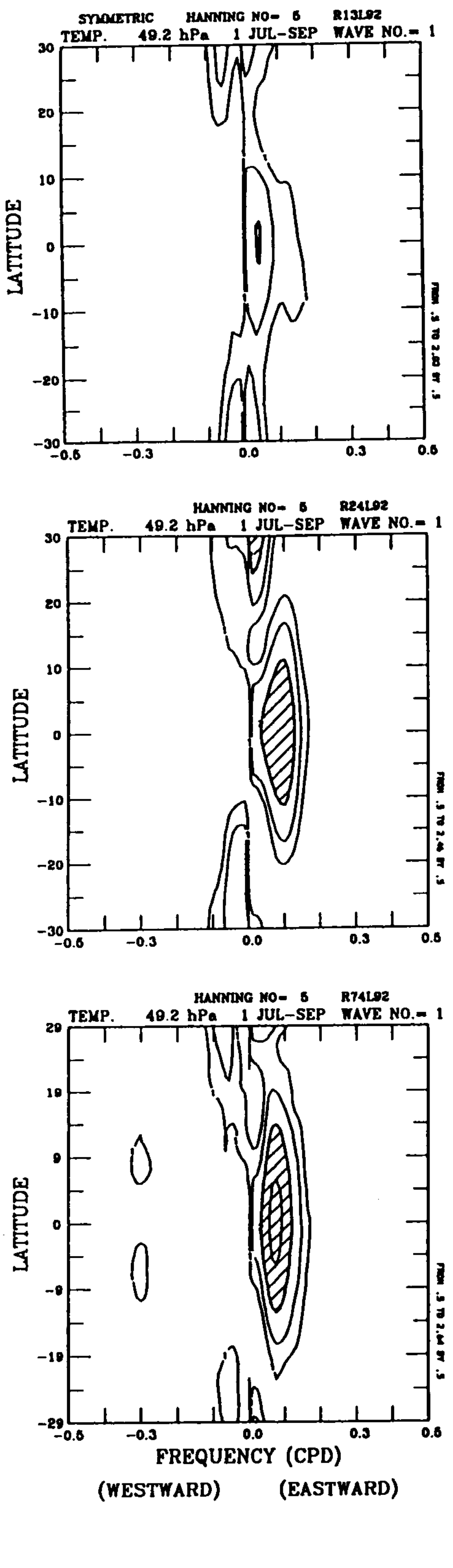

Figure 2. Power spectrum of temperature wave 1 in frequency-latitude plane at 49.2 hPa during Jul, Aug and Sep for R13(upper), R24(middle) and R74(lower).

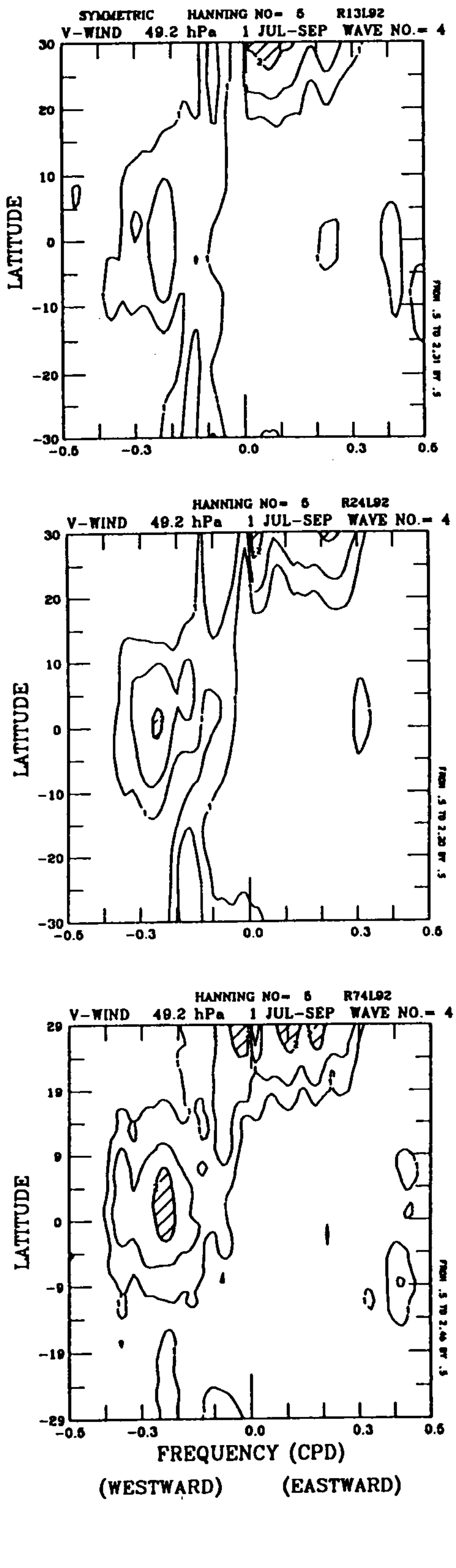

Figure 3. The same as in Figure 1 except for meridional wind of wave 4 during Sep, Oct and Dec.

small and the wave of about 5 km vertical wavelength maximizes in this height, while R24L92 and R74L92 models show much larger power with a maximum value for the wave of about 10 km vertical wavelength. Comparison between the middle and upper stratosphere (not shown) reveals that the high power region largely shifts toward longer vertical wavelength (higher frequency) with height in R13L92 model, but that slight shifts occur in R24L92 and R74L92 models.

Figure 3 shows the latitudinal distribution of the power of wave number 4 meridional winds, in which westward propagating waves are the mixed Rossby-gravity waves, for the period from October to December. The power of around 5-day period, which corresponds to the peak value in Figure 3, increases in R24L92 and R74L92 models. Nevertheless, the power in R24L92 model is slightly larger than that in R74L92 model, whereas the former is smaller than the latter near the tropopause. This indicates that the dissipation of the mixed Rossby-gravity waves in R74L92 model is larger than that in R24L92 model, being consistent with the evolution of the zonal-mean zonal wind in Figure 1. The difference in the simulated equatorial stratosphere therefore is resulted from that the horizontal resolution increase makes more favorite conditions for upward propagation of the equatorial waves.

4. Conclusion of off-line transport experiment

4.1 R24L92 Model

Passive tracer transport experiments are made using the R24L92 simulated winds data sampled every 2 hours. Ten thousand particles are used as tracers and their trajectories are calculated with time step of one hour. Initially, one thousand particles are isotropically distributed in a box region of 1 by 1, extended from 200 to 150 hPa, and ten boxes are located equally-spaced, 36 apart from adjacent boxes, on the equator. Two initial dates, June 1st and December 1st, are used and time integrations are made for 2 months.

The trajectories of the particles, which are situated higher than 70 hPa, which is in the over-world (Hoskins, 1991), on the last day, are shown in Fig.4. The two panels, though there are different features, show a prominent common feature that major cross-tropopause transport occurs not in the vicinity of the equator but in 10-20 latitude regions. Cross-isentrope transport is due to updraft, which is diabatic heating in the isentropic coordinates (Andrew et al., 1987). Meridional cross section of diabatic heating show that maximum axes is around 25 degrees in the middle and lower stratosphere, being different from the trajectories in Figure 4.

Figures 5 and 6 show the over-world particle trajectories projected into the horizontal surface (upper panel), and wind and diabatic heating (lower panel) on 370 K isentrope, which coincides with the thermal tropopause in the tropics. Comparison between both panels indicates that major upward transport regions are corresponding to the regions, where both conditions of very weak wind and large diabatic heating are fulfilled.

4.2 R74L92 Model

Similar transport experiments of 2 months integration are made with R74L92 using two and half years data. The major results are as follows: (1) In northern summer and autumn the cross-tropopause transport in low-latitudes shows non-symmetric pattern with respect to the equator, and it is much larger in southern hemisphere than in northern hemisphere; (2) In winter and spring the transport is nearly symmetric; (3) The particle number transported into the stratosphere is the smallest in summer, intermediate in autumn and winter, and the largest in spring with the ration spring to summer exceeding 3; (4) there are favorable regions for the transport, where large diabatic heating and weak wind are both occurred.

References

Andrew, D. G., J. R. Holton and C. B. Leovy, 1987: Middle Atmosphere Dynamics, Academic Press, 489 pp.

Holton, J. R., P. H. Haynes, M. E. McIntyre, A. R. Douglass, R. B. Rood and L. Pfister , 1995: Stratosphere-troposphere exchange. Rev. Geophys., 33, 403-439.

Hoskins, B. J., 1991: Towards a PV-theta view of the general circulation. Tellus, A43, 27-35.

Shibata, K and M. Chiba, 1990: A simulation of seasonal variation of the stratospheric circulation with a general circulation model. J. Meteorol. Soc. Japan, 68, 687-703.

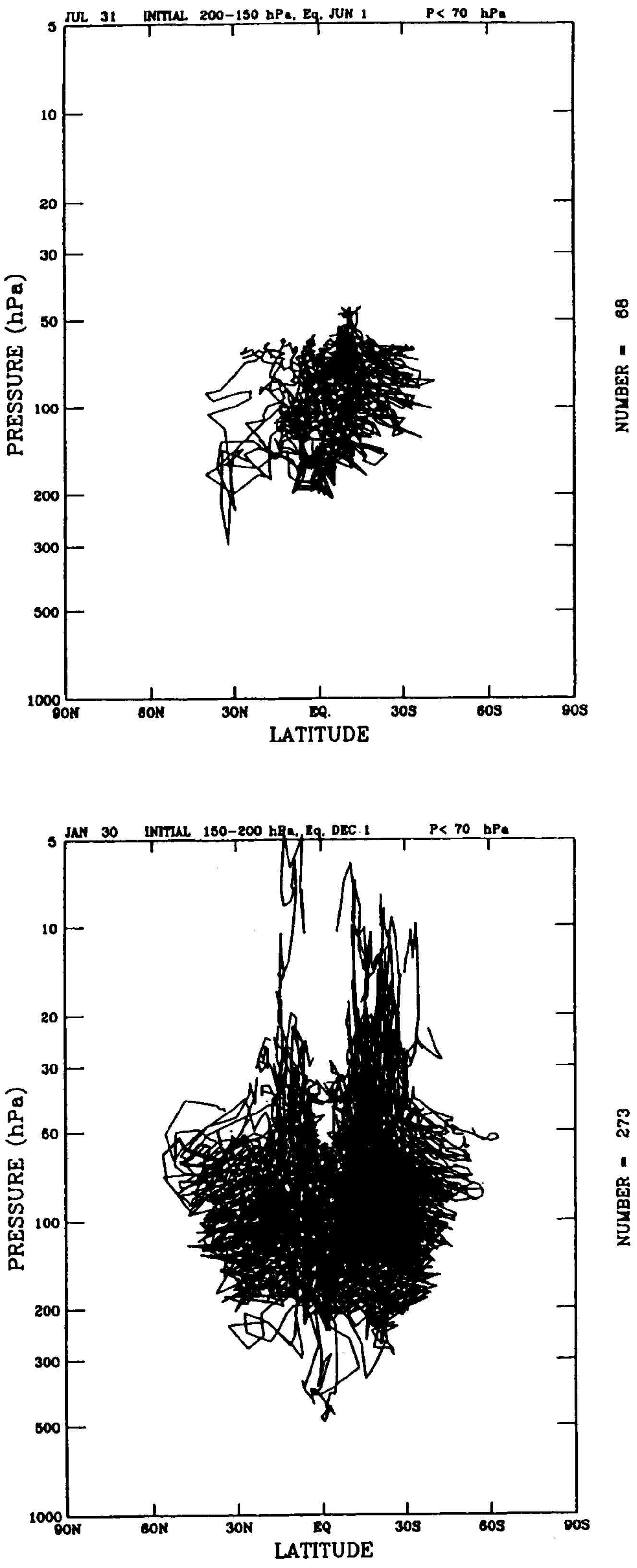

Figure 4. Trajectories projected on the meridional section for the the particles situated higher than 300 hPa after two months integration on July 31(upper) and on January 31(lower).

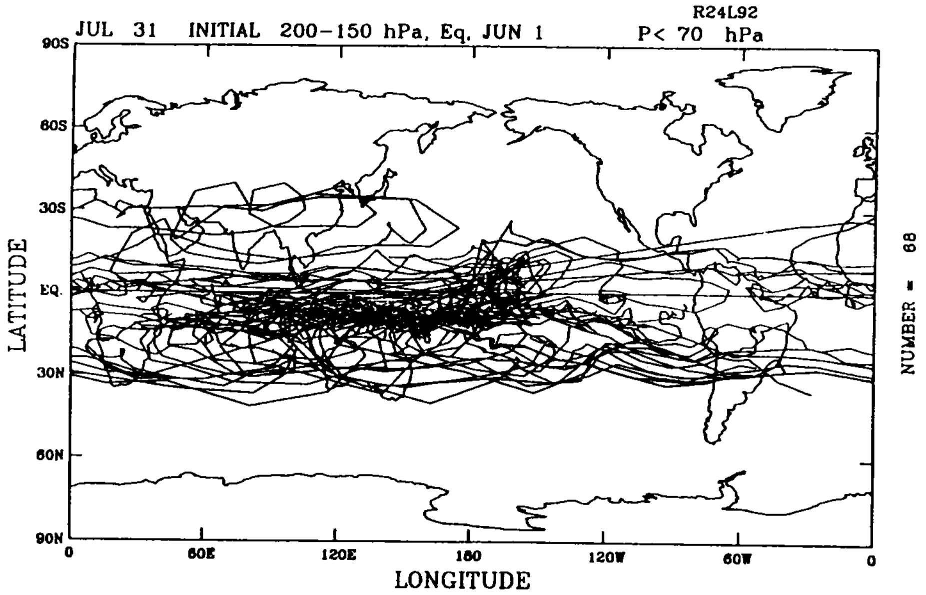

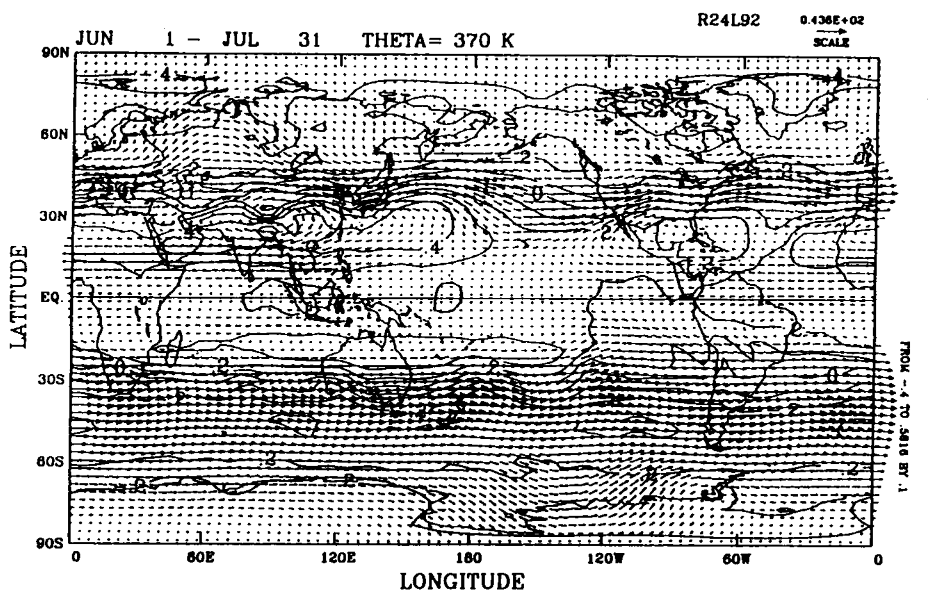

Figure 5. Trajectories projected on the geographical plane for the the particles situated higher than 70 hPa on July 31(upper) and wind and diabatic heating(lower, contour interval is 0.1 K/day).

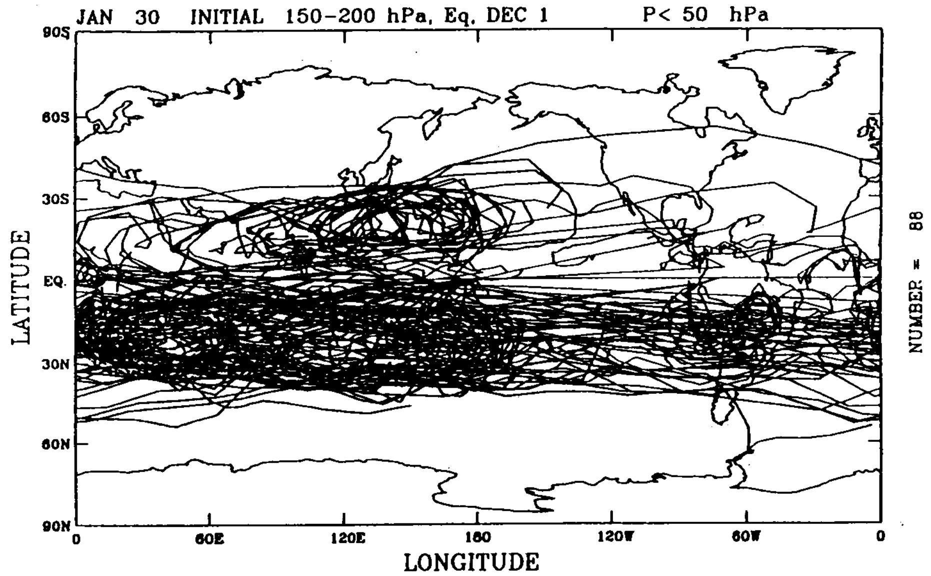

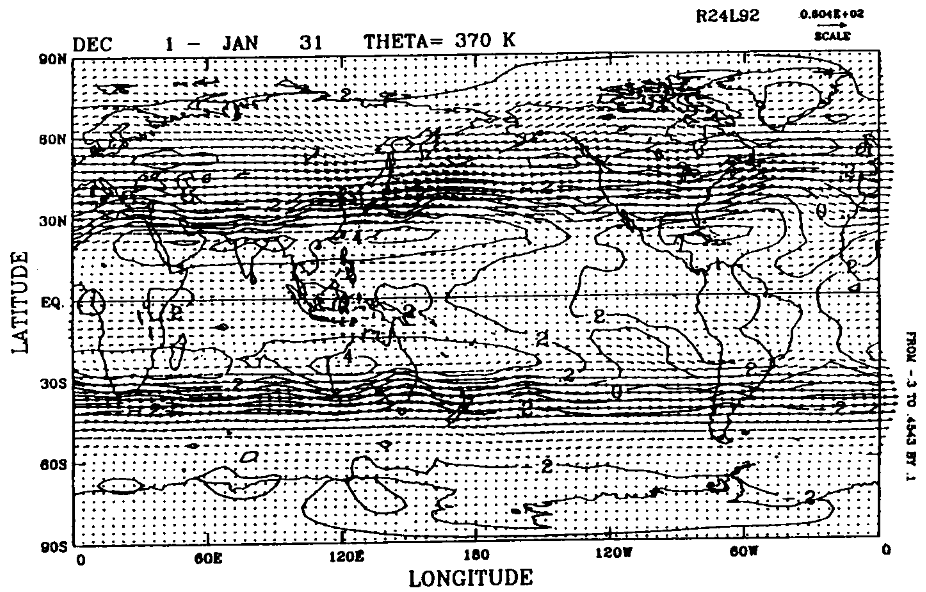

Figure 6. The same as in Figure 5 except for 50 hPa for trajectories.